Cellular 4G LTE MIMO Antenna System Modeling Utilizing Measured Vehicle-Level Antenna Patterns

Daniel N. Aloi, Jia Li and Esosa Ekhoragbon
Electrical and Computer Engineering Department
Oakland University
Rochester, Michigan, USA
{aloi, li4, esosaekhoragbon}@oakland.edu

Leo Lanctot and John Locke
RF Antenna Systems
Ford Motor Company
Dearborn, Michigan, USA
{llanctot, jlocke16}@ford.com

2021 Antenna Measurement Techniques Association Symposium (AMTA) | 978-1-7362351-1-9/21/$31.00 ©2021IEEE 23919/AMTA52830.2021.9620715

***Abstract*— Cellular LTE MIMO downlink performance, for 4x4, 4x2, and 2x2 LTE MIMO architectures, in terms of average data throughput and availability, were investigated in an urban canyon environment of Frankfurt, Germany at 2110 MHz on a Sport Utility Vehicle (SUV) with metal and glass roofs for a virtual route. This study utilized the following measured antenna radiation patterns for total polarization on the SUV at 2110 MHz for the mobile station: 1) roof-mounted antenna on metal roof; 2) roof-mounted antenna on glass roof; 3) interior-mounted planar-inverted F antenna; and 4) interior-mounted planar-inverted F antenna rotated 90 degrees. This research was carried out using a three-dimensional simulation software suite that enabled users to simulate electromagnetic wave propagation and wireless network planning.**

The following observations were obtained from this research. First, the MIMO architectures for the SUV with metal roof exhibited approximately 5% higher average data throughput levels compared to the same MIMO architectures on the SUV with glass roof. Second, the throughput availability for the 4x4 and 4x2 MIMO systems were comparable. Lastly, the average throughput for the 4x4 MIMO system was higher than the 4x2 and 2x2 MIMO systems for the SUV regardless of roof material.

I. Introduction

With the automotive industry supporting connectivity applications including over-the-air (OTA) software updates and data analytics, cellular service is required. The automotive connectivity applications require the vehicle to meet the new cellular performance specifications that are tailored to mobile handsets as opposed to vehicles. Release 15 of the 5G 3GPP Standard will increase the number of shark-fin type antennas on a vehicle in order to reap the benefits of the multiple-input-multiple-output (MIMO) technology including higher channel capacity, higher data throughput, and lower latency.

A better understanding of vehicle cellular performance may allow freedom to use different and unique antenna designs and placements. Better insight will lead to improved styling and cost reductions while maintaining the quality of the connectivity features.

This paper is specifically focused on sub-6GHz cellular LTE and 5G which is the RF systems that has the greatest influence on number and size of antennas. MIMO antenna system performance is assessed on a sport utility vehicle (SUV) with a metal and a glass roof utilizing various antenna configurations.

This research includes models to assess MIMO performance on virtual routes (Ray Tracing Software – Altair's WinProp). The focus is on an urban environment in which MIMO is most effective.

This paper is organized as follows. Section II describes the virtual scenario used to assess the different MIMO architectures and includes descriptions of the virtual environment and route, the mobile station (MS) and base station (BS) settings, and the vehicle-level antenna patterns used in these analyses. Section III contains the results for the MIMO architecture studies. And Section IV states the observations of this research.

II. Virtual Scenario

A baseline scenario was created with a commercial off the shelf software (COTS) suite that enables users to simulate electromagnetic wave propagation and wireless network planning. The following sections describe the details of the baseline scenario to assess cellular 4G Long Term Evolution (LTE) MIMO performance for various MIMO architectures as a function of their associated antenna patterns on MIMO data throughput performance and availability for a MS, a vehicle in this work, in an urban canyon environment for a cellular LTE network for a virtual route.

A. Urban Canyon Environment

Figure 1. shows the urban canyon database for Frankfurt, Germany in top view and 3D isometric views in subplots a) and b), respectively. The statistics for the objects in this urban canyon database are provided in Table I.

Figure 1. Urban canyon model of Frankfurt, Germany: a) Top View and b) 3D isometric view.

TABLE I. STATISTICS FOR OBJECTS IN URBAN CANYON DATABASE FOR FRANKFURT, GERMANY.

Total Number of Objects	683
Number of Standard Buildings	683
Number of Horizontal Plates	0
Number of Courtyards/Towers	0
Number of Vegetation Blocks	0
Number of Virtual Buildings	0
Corners	
Mean Number of Corners Per Object	7.11
Maximum Number of Corners	29
Height	
Minimum	0.00 meters
Maximum	191.25 meters

The frequency dependent material properties for the 683 buildings of the urban canyon database of Frankfurt, Germany are shown in Table II.

TABLE II. FREQUENCY DEPENDENT MATERIAL PROPERTIES FOR URBAN CANYON DATABASE OF FRANKFURT, GERMANY.

Transmission/Reflection/Scattering	
Transmission Loss	20.5 dB
Reflection Loss	6 dB
Scattering Loss	20 dB
Diffraction	
Incident (Minimum)	8 dB
Incident (Maximum)	15 dB
Diffracted	5 dB
Electrical Properties	
Relative Permittivity	4.0
Relative Permeability	1.0
Conductivity	0.01 S/m

Topography, vegetation areas, court yards, and towers can also be added to urban databases. However, none of those features were added to the urban database of Frankfurt, Germany in this study.

B. *Propagation Model*

The Standard Intelligent Ray Tracing (IRT) propagation model was used to determine the wave propagation characteristics between the cellular BS and the MS in the urban canyon environment. The IRT is a ray-tracing algorithm that takes into account direct rays, reflected rays and diffracted rays. Furthermore, they consider up to 3 combinations of these interactions when determining the received signal strength at the MS [1].

C. *Cellular Air Interface Settings*

A cellular MIMO LTE network was simulated for the urban canyon environment of Frankfurt, Germany with the following parameters defined in Table III.

TABLE III. CELLULAR LTE AIR INTERFACE SETTINGS FOR VARIOUS MIMO ARCHITECTURES.

Multiple Access	OFDM / SOFDMA
Duplex Separation	Duplex FDD with 190 MHz separation
MIMO	
Number of data streams	2 or 4
Interference between MIMO streams	None
	Relative contribution Location dependent
Carriers for Downlink	
Carrier ID	25
Frequency	2112.5 MHz
Transmission Mode Parameters - Downlink	
Modulation	256-QAM
Code Rate	4/5
Nr of resource blocks	1
Overhead ratio	0%
Data rate	1.08 Mbit/s

In these simulations, performance of the downlink channel was considered. The interference between MIMO data streams is an important parameter that impacts the data throughput results in these simulations. The interference between data streams was not taken into account in this study.

D. *Base Station*

A single base station site was selected for all scenarios and is illustrated in the center of the city at a height of 80 meters in Figure 2. The number of transmitting antennas depended on the number of MIMO data streams. The following MIMO architectures were simulated in this study: 1) 4x4 MIMO with 4 data streams; 2) 2x2 MIMO with 2 data streams; and 4) 4x2 MIMO with 2 redundant data streams. For all cases, the transmitting antennas were arranged in a linear array with 0.3 meters spacing between them. All of them were at the same height of 80 meters. An omni-directional radiation pattern was chosen for each BS antenna for total polarization at a frequency of 2110 MHz.

Figure 2. Urban canyon scenario with base station located in center of city at a height of 80 meters.

For each transmit antenna, the transmission power level, assigned downlink carrier frequency and MIMO data stream number are assigned. In each of these scenarios, transmission power levels of 0 dBm, 10 dBm, 20 dBm, 30 dBm, and 40 dBm were used. They can be mapped to a signal-to-noise level (SNL) at the MS since the path loss and atmospheric noise are know from the simulations.

E. Mobile Station

The MS locations were defined for a virtual route with 13,048 independent points along the trajectory spaced 1.0 meters apart from each other at a height of 1.5 meters relative to the ground. This was a static scenario indicating the velocity of the MS at each pixel was 0.0 m/s. The virtual route is the red line shown in Figure 2.

The following characteristics of the MS receiver are listed in Table IV.

TABLE IV. DEFINED PARAMETER FOR THE MS RECEIVER.

Minimum Sensitivity	-93 dBm
SINR	10 dB
NF	6 dB
Power Summation Method	Coherent using amplitude and phase of each ray contribution during summations

The number of receiving antennas on the MS were dependent on the MIMO architecture. The 2x2, 4x2 and 4x4 MIMO architectures were implemented with either 2 or 4 receiving antennas on the MS. The physical three-dimensional locations for each receiving antenna are defined by the user. Furthermore, the on-vehicle measured radiation patterns for each antenna were imported into the COTS software package for a particular polarization and physical location on the MS platform.

F. Key Performance Indicators

Data throughput was the main metric used to assess the performance of each MIMO architecture. Specifically, the average data throughput and data throughput availability percentage for the 13,048 potential locations throughout the vehicle trajectory were computed based on (1) and (2), respectively.

$$T_{avg} = \frac{\sum_{i=1}^{N} T_i}{N} \quad (1)$$

$$T_{availability} = \frac{N - \sum_{i=1}^{N} (T_i = 0)}{N} \quad (2)$$

where T_{avg} is the average throughput, T_i is the throughput at location i, and N is the total number of locations (13,048 in this case). The throughput availability percentage formula uses the variable $T_{availability}$ for the percentage of locations with non-zero T_i values.

III. SUV – MIMO ARCHITECTURE STUDY

This study compares a 4x4 MIMO system with 2 roof-mounted antennas (good radiation pattern characteristics) and 2 interior-mounted antennas (marginal radiation pattern characteristics) against a 4x2 and 2x2 MIMO systems with 2 roof-mounted antennas (good radiation pattern characteristics). The BS antennas were slant-linear polarized omni-directional antennas arranged in a linear array with 2λ spacing at 2110 MHz while total polarization was used for the MS antennas (i.e. complex radiation pattern for VLP and HLP). The BS transmit power levels ranged from 0 dBm to 40 dBm in 10 dB increments and their data stream assignments are shown in Table V. An overview of the BS station antenna types and assignments are shown in Table VI.

TABLE V. BS DATA STREAM ASSIGNMENTS.

Case Number	*MIMO*	*Ant. 1*	*Ant. 2*	*Ant. 3*	*Ant. 4*
1.	4x4	Data Stream 1	Data Stream2	Data Stream3	Data Stream4
2.	4x2	Data Stream 1	Data Stream2	Data Stream1	Data Stream2
3.	2x2	Data Stream 1	Data Stream2	----	----

TABLE VI. MS SIMULATION PARAMETERS FOR 4X4,4X2 AND 2X2 MIMO SYSTEMS AT 2110 MHZ INTEGRATED ON A LARGE SUV WITH METAL AND GLASS ROOFS.

Case Number	*MIMO*	*Roof Type*	*Ant. 1*	*Ant. 2*	*Ant. 3*	*Ant. 4*
1.	4x4	Metal	Roof1	Roof2	PIFA1	PIFA2
2.	4x2	Metal	Roof1	Roof2		
3.	2x2	Metal	Roof1	Roof2		
4.	4x4	Glass	Roof1	Roof2	PIFA1	PIFA2
5.	4x2	Glass	Roof1	Roof2		
6.	2x2	Glass	Roof1	Roof2		

The locations of the four MS antennas for the 4x4 MIMO architecture are shown in Table VII. The 4x2 and 2x2 MIMO architectures removed the PIFA antennas and used the same locations for the two roof antennas. Ideal separation between data streams was assumed for this study (i.e. ECC was ideal).

TABLE VII. MS ANTENNA LOCATIONS FOR 4X4 MIMO SYSTEM.

	X (m)	Y (m)	Z (m)
Roof 1	-0.5	-0.375	+1.5
Roof 2	-0.5	+0.375	+1.5
PIFA1	+0.5	-0.0375	+1.25
PIFA2	+0.5	+0.0375	+1.25

The three-dimensional radiation patterns for total polarization for the two roof antennas and two interior-mounted PIFA antennas at 2110 MHz are shown in Figure 3 where subplot a) is the PIFA1; subplot b) is the PIFA2 rotated 90°; subplot c) is the roof-mount antenna on glass roof; and subplot d) is the roof-mount antenna on a metal roof.

Table VIII. shows the linear average gain at both individual theta angles as well as over a range of 30° (i.e. 60°-90° where 90° is the antenna horizon) for the glass roof and the metal roof. The last row in Table VIII. shows a delta between the linear average gain of the roof antenna relative to the linear average gain of the PIFA antenna for the glass roof and the metal roof with values of +3.0 dB and +3.9 dB, respectively. These values were computed from the gain measurements in Figure 3. These differences can be thought of as a channel imbalance in a statistical sense but are not necessarily the same as channel imbalance due to differential cable length which would be a bias.

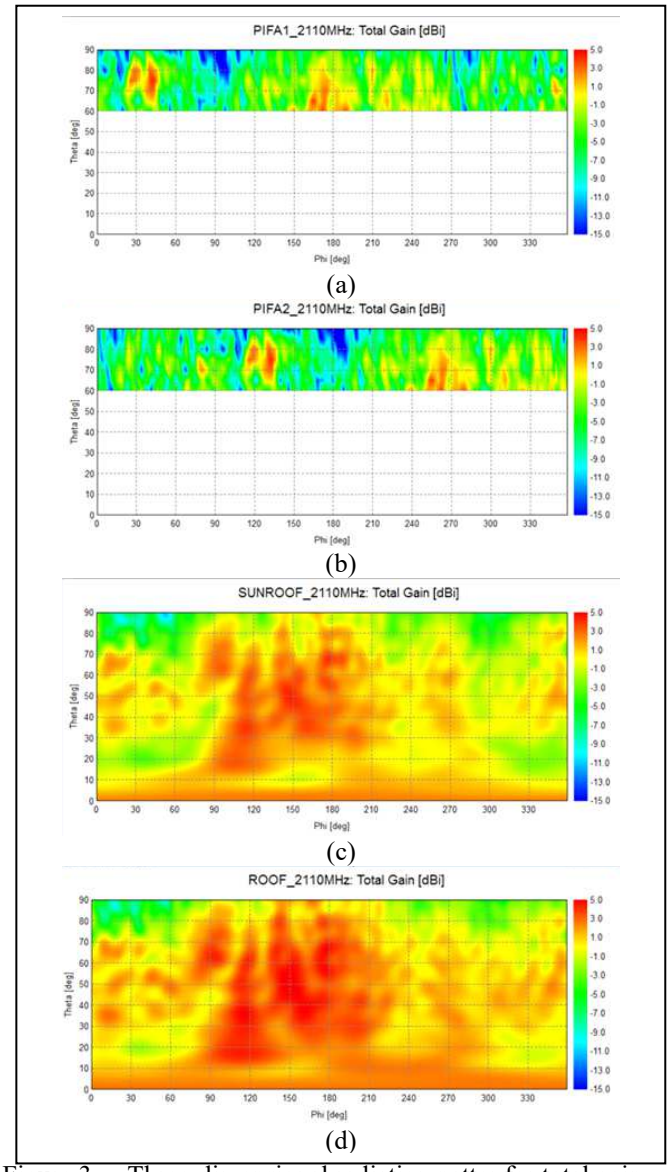

Figure 3. Three-dimensional radiation patter for total gain at 2110 MHz for roof-mounted and interior-mounted antennas on large SUV with glass roof and metal roof.

TABLE VIII. STATISTICAL COMPARISON OF LINEAR AVERAGE GAIN FOR A ROOF MOUNTED ANTENNA AND INTERIOR-MOUNTED ANTENNA ON A LARGE SUV WITH METAL ROOF AND GLASS ROOF.

	Glass Roof			Metal Roof		
THETA (deg)	***ROOF (dBi)***	***PIFA (dBi)***	***DELTA (dB)***	***ROOF (dBi)***	***PIFA (dBi)***	***DELTA (dB)***
60	+0.3	-3.0	+3.3	+1.3	-3.0	+4.3
70	+0.0	-2.6	+2.6	+0.9	-2.6	+3.5
80	-1.0	-3.5	+2.5	-0.1	-3.5	+3.4
90	-2.7	-6.8	+4.1	-1.6	-6.8	+5.2
60-90	-0.6	-3.6	+3.0	+0.3	-3.6	+3.9

Figure 4. shows the angle of arrival (AoA) for all of the position locations along the virtual route relative to the BS. The AoA are predominantly between 60°-90° in theta emphasizing the importance of this range of angles for the antenna pattern statistics provided in Table VIII.

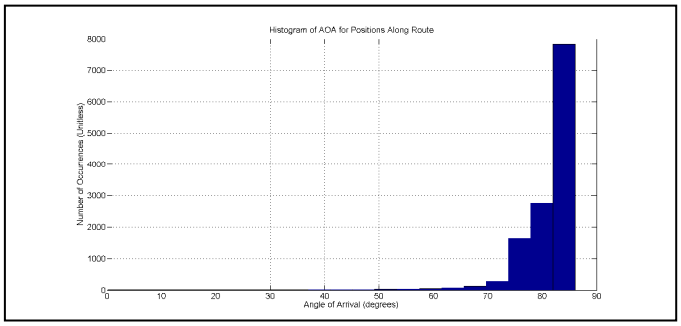

Figure 4. Histogram of AoA along virtual route to MS relative to BS.

A. Throughput Results for Glass Roof SUV

Figure 5. shows the average throughput results for 4x4, 4x2 and 2x2 MIMO antenna configurations on a large SUV with a glass roof. The following observations are made for Figure 5. at transmit power levels above 30 dBm:

- The 4x4, 4x2 and 2x2 MIMO systems exhibited average throughput values of 38 Mbps, 31 Mbps, and 24 Mbps, respectively.
- The average throughput of the 4x4 MIMO system performed worse than the 4x2 MIMO system at transmit power levels below 17 dBm.

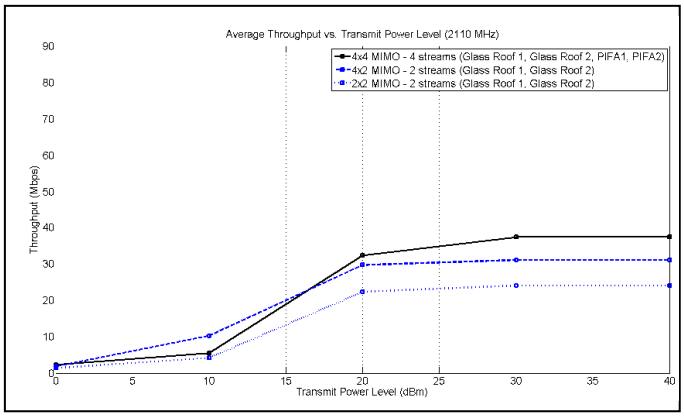

Figure 5. Average throughput vs. transmit power level for vehicle with glass roof at 2110 MHz for three MIMO architectures.

The throughput availability percentage vs transmit power level for the three MIMO architectures for the large SUV with glass roof are shown in Figure 6.

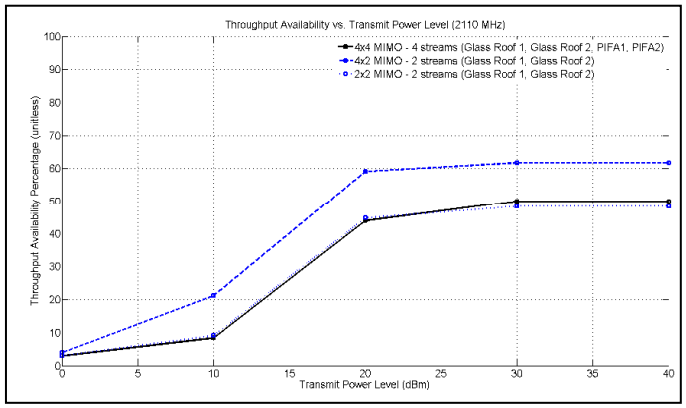

Figure 6. Throughput availability percentage vs. transmit power level for vehicle with glass roof at 2110 MHz for three MIMO architectures.

The following observations are made:

- The 4x2 MIMO system exhibited the highest availability percentage for all transmit power levels relative to the 4x4 and 2x2 MIMO systems.
- The availability percentage for the 4x4 and 2x2 MIMO systems were within 1% of each other for all transmit power levels.

B. Throughput Results for Metal Roof SUV

Figure 7. shows the results for the 4x4, 4x2 and 2x2 MIMO antenna configurations on the large SUV with a metal roof. The following observations are made for Figure 7. above 30 dBm transmit power level:

- The 4x4, 4x2 and 2x2 MIMO systems exhibited average throughput values of 38 Mbps, 31 Mbps, and 24 Mbps, respectively.
- The average throughput of the 4x4 MIMO system performed worse than the 4x2 MIMO system at transmit power levels below 17 dBm.

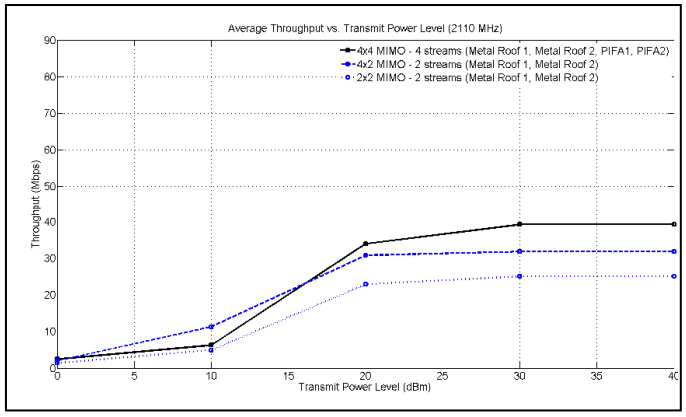

Figure 7. Average throughput vs. transmit power level for vehicle with metal roof at 2110 MHz for three MIMO architectures.

The throughput availability percentage vs transmit power level for the three MIMO architectures for the large SUV with glass roof are shown in Figure 8.

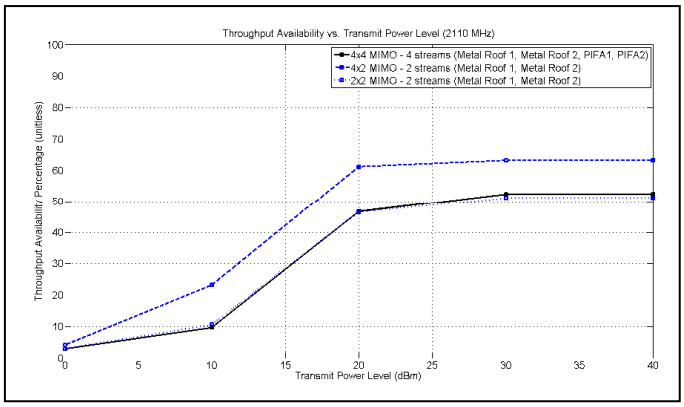

Figure 8. Throughput availability percentage vs. transmit power level for vehicle with metal roof at 2110 MHz for three MIMO architectures.

The following observations are made:

- The 4x2 MIMO system exhibited the highest availability percentage for all transmit power levels relative to the 4x4 and 2x2 MIMO systems.
- The availability percentage for the 4x4 and 2x2 MIMO systems were within 1% of each other for all transmit power levels.

A summary is provided in Table IX. at a transmit power level of 40 dBm in order to compare the performance metrics (average throughput and throughput availability percentage) and the roof type (glass or metal) of the large SUV.

TABLE IX. SUMMARY OF AVERAGE THROUGHPUT AND THROUGHPUT AVAILABILITY FOR LARGE SUV WITH GLASS AND METAL ROOF AT TRANSMIT POWER LEVEL OF 40 DBM.

	Glass Roof		**Metal Roof**	
	Average Throughput (Mbps)	***Throughput Availability (%)***	***Average Throughput (Mbps)***	***Throughput Availability (%)***
4x4	38.0	52.0	39.0	53.0
4x2	31.0	62.0	32.0	64.0
2x2	24.0	50.0	25.0	51.0

First, large SUV with metal roof had slightly higher performance in both performance metrics over the large SUV with glass roof. Next, for both roof types, the 4x4 MIMO system had the highest average throughput while the 4x2 MIMO system had the highest availability percentage.

IV. CONCLUSIONS

The following observations were made in this study in regards to material of vehicle roof and the use of 2 good antennas and 2 marginal antennas in a 4x4 MIMO system:

- The large SUV with metal roof exhibited average throughput values vs. transmit power levels that

were approximately 2% higher than those for the Large SUV with glass roof.

- The throughput availability percentage (i.e. number of locations with no throughput) was highest for the 4x2 MIMO system followed by the 4x4 and 2x2 MIMO systems were comparable in performance to each other but about 20% lower than the 4x2 MIMO system which was attributed to the two redundant data stream transmissions at the BS.
- The average throughput for the 4x4 MIMO system was higher than the 4x2 and 2x2 MIMO systems.

These results are interesting for automotive original equipment manufacturers (OEMs) as to whether it is financially worth adding two additional interior-mounted antennas on a vehicle (i.e. MS) in a cellular LTE or 5G network in order to attain higher average throughput performance albeit slightly less throughput availability performance. It is worth noting this study only included an urban canyon scenario and does not represent all driving environments.

ACKNOWLEDGEMENT

The authors would like to thank Ford Motor Company for funding this research effort and providing the measured radiation patterns for the exterior and interior mounted antennas on the large SUVs with glass and metal roof. In addition, the authors would like to thank Oakland University graduate student Akram Awad for his help in running simulations.

REFERENCES

[1] Altair, *Altair WinProp 2019.3 User Guide,* Troy, Michigan: Altair2002020.